Endoplasmic Reticulum Targeting Ratiometric Fluorescent Probe for Carboxylesterase 2 Detection in Drug-induced Acute Liver Injury

Xiangge Tian, [†,#] Fei Yan, [†,‡,#] Jingyuan Zheng, [†,#] Xiaolin Cui, [†] Lei Feng, [†,*] Sheng Li , [†] Lingling Jin , [†] Tony D. James [§,*] and Xiaochi Ma [†,‡,*]

[†] Academy of Integrative Medicine, National-Local Joint Engineering Research Center for Drug-Research and Development (R&D) of Neurodegenerative Diseases, College of Pharmacy, Dalian Medical University, Lvshun South Road No 9, Dalian 116044, China;

[‡] Jiangsu Key Laboratory of New Drug Research and Clinical Pharmacy, Xuzhou Medical University, 209 Tongshan Road, Xuzhou, 221004, Jiangsu, China;

[§] Department of Chemistry, University of Bath, Bath, BA2 7AY, UK.

ABSTRACT: Carboxylesterase 2 (CES2) an endoplasmic reticulum (ER) located phase I enzyme plays a vital role in the metabolism of various endogenous and exogenous substances, and is regarded as an important target for the design of prodrugs. Unfortunately, superior highly selective ER targeting fluorescent probes for monitoring of CES2 are not currently available. Herein, we report an ER targeting CES2 selective and sensitive ratiometric fluorescent probe **ERNB** based on the ER localizing group *p*-toluenesulfonamide. **ERNB** possessed high specificity, sensitivity, and exhibited excellent subcellular localization when compared with commercial ER tracker, and was used to image CES2 in the ER of living cells. Additionally, using **ERNB** we evaluated the CES2 regulation under DL-dithiothreitol and tunicamycin-induced ER stress. Furthermore, we determined the down regulation of CES2 activity and expression in the acetaminophen-induced acute liver injury model. Based on these results we conclude that **ERNB** is a promising tool for highlighting the role of CES2 in the ER and in exploring the role of CES2 in the development of diseases associated with ER stress.

INTRODUCTION

Carboxylesterase 2 (CES2) an important phase I metabolic enzyme plays a vital role in the metabolism of various endogenous substrates such as acyl-CoA, acylcarnitine, cholesterol ester etc., it is also responsible for the detoxification of clinical drugs, and can activate many prodrugs such as anti-tumour drugs irinotecan (CPT-11) and capecitabin, narcotics (cocaine, heroin and meperidine) and methylphenidate.[1-5] Thus, CES2 is regarded as a molecular target for prodrugs.[5] Furthermore, CES2 has been shown to be important in several critical diseases, for instance, CES2 can prevent liver steatosis by modulating lipolysis, endoplasmic reticulum (ER) stress; and reverse obesity-induced diacylglycerol accumulation and glucose intolerance.[4] In mammals, CES2 locates in the ER and is expressed in several organs including liver, intestine, and kidney.[6,7] Notably, the expression of CES2 shows inter-individual variation in the clinic and can be regulated by several mechanisms, such as gene polymorphism and epigenetic processes. ER stress usually occurs during pathological states including liver injury, inflammation, obesity, drug-induced toxicity etc.,[8-14] and has received wide attention due to its role in drug metabolism and human diseases.[15-17] However, changes of CES2 located in the ER associated with stress, have not been fully evaluated. Therefore, it is of great importance to develop a sensitive and specific method for the real-time detection of endogenous endoplasmic reticulum CES2 for various disease diagnoses and therapies.

Fluorescence imaging technology with its numerous advantages, such as good sensitivity, real-time detection, high spatiotemporal resolution, and non-invasive monitoring ability in living systems has been widely applied in various diseases diagnoses and therapies.[18-26] Fluorescent probes for monitoring CES2 have been developed for tissues and cell preparations;[27-32] however, measuring CES2 in the ER during some ER-associated diseases has been limited, since none of the CES2 fluorescent probes to date are ER targeting.

Herein, we designed and developed an ER targeting ratiometric fluorescent probe (**ERNB**) for CES2 detection based on the substrate preferences of CES2. Targeting was achieved by introducing a well-known ER-targeting group *p*-toluenesulfonamide (**Scheme 1**).[33-36] **ERNB** exhibited high selectivity and sensitivity toward CES2 and could image endogenous CES2 in cells and tissues. Furthermore, **ERNB** displayed excellent ER-targeting ability and exhibited exceptional colocalization with commercial ER tracker. Additionally, **ERNB** indicated that the activity of CES2 was significantly reduced under DL-dithiothreitol (DTT) and tunicamycin-induced ER stress in an acute liver injury model.

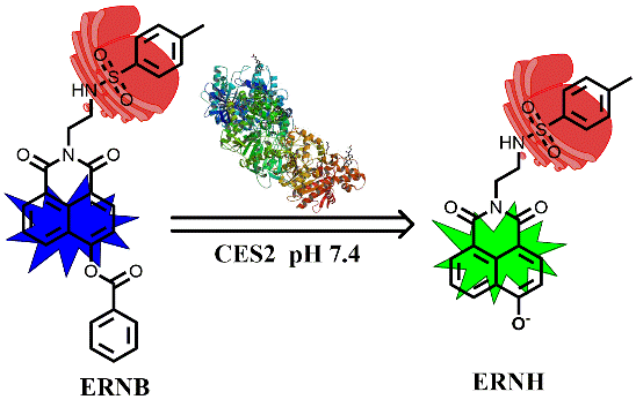

Scheme 1 The structure and mechanism of ER targeting fluorescent probe **ERNB** for the detection of CES2.

EXPERIMENTAL SECTION

Materials and instruments. Different metabolic enzymes including: Carboxylesterases (CES1, CES2), *β*-galactosidase (*β*-Gla), Lysozyme (Ls), Carbonic anhydrase (Cas), *β*-glucuronidase (*β*-Glu), *β*-glucosidase (*β*-Glc) and Human serum albumin (HSA) were purched from Sigma-Aldrich (St Louis, MO). L (+)-Cysteine, Myristic acid, Tryptophan, Tyrosine, Serine, Glutanic acid, Glutathione, Glycine, Lysine, L-Arginine, Glutamine, and Glucose were all purchased from Shanghai yuanye (Shanghai, China). ER-tracker Red (BODIPY ® TR Glibenclamide) is purchased from Shanghai Yisheng (Shanghai, China). HepG2 cells were purchased from American Type Culture Collection (Manassas, VA). HepG2 cells were purchased from American Type Culture Collection (Manassas, VA). CES2 and *β*-actin antibodies were obtained from Abcam. All fluorescence tests performed on Synergy H1 Hybrid Multi-Mode Microplate Reader (BioTek). NMR spectra were obtained using Bruker Avance II (400 MHz) spectrometer. Accurate mass detection was measured on G6224A TOF MS. The HPLC analysis was conducted on the Waters e2695 equipped with 2998 PDA Detector. All other reagents and solvents used were of the highest grade commercially available.

Synthesis pathway for ERNB

Synthesis of ERNH. 4-hydroxy-1, 8-naphthalic anhydride (107.0 mg, 0.50 mmol) and *N*-tosylethylenediamine (117.7 mg, 0.55 mmol) were dissolved in ethanol (30 mL). The reaction mixture was stirred and refluxed for 24 h. After cooling to room temperature, the solvent was removed *in vacuo*, and the residual solid was purified by 2767 Waters Prominence HPLC system equipped with a Waters 2767 sample manager, and a Waters 2545 binary Gradient Module, a Waters 2489 UV/Visible Detector and a Waters X Bridge C18 (19 mm × 150 mm, 5 μm) chromatograph column. The preparative liquid phase: mobile phase contained A (100% methanol) and B (Trifluoroacetic acid water containing 10% methanol), the elution process was Isometric elution and the mobile phase was 60% (A): 40% (B).) Affording **ERNH** 49.2 mg. (Yield 24%). ^{1}H NMR (400 MHz, DMSO-d_6) δ 11.86 (s, 1H), 8.54 (d, J = 8.3 Hz, 1H), 8.44 (d, J = 7.3 Hz, 1H), 8.32 (d, J = 8.2 Hz, 1H), 7.74 (dt, J = 12.3, 7.0 Hz, 2H), 7.59 (d, J = 7.5 Hz, 2H), 7.22 (d, J = 7.8 Hz, 2H), 7.16 (d, J = 8.2 Hz, 1H), 4.09 (t, J = 6.4 Hz, 2H), 3.06 (q, J = 6.3 Hz, 2H), 2.26 (s, 3H). ^{13}C NMR (100 MHz, DMSO-d_6) δ 164.26, 163.55, 160.70, 142.87, 138.10, 133.98, 131.55, 129.91, 129.79, 129.33, 126.82, 126.05, 122.84, 122.37, 113.17, 110.36, 40.63, 39.46, 21.33. HRMS (ESI negative) calcd for $[M-H]^-$ 409.0864, found 409.0871. (**Figure S1**-**S5**).

Synthesis of ERNB. To a solution of **ERNH** (41 mg, 0.10 mmol) and Et_3N (28 μL, 0.20 mmol) in 10 mL of DMF, benzoyl chloride (18 μL, 0.15 mmol, mixed with 1 mL of DMF) was added dropwise at 0 °C over 15 min. After stirring at this temperature for 1 h, the mixture was warmed to room temperature and stirred overnight. The solvent was removed, and the residual solid was purified by preparative HPLC as mentioned above and the isometric mobile phase was set with 70% (A): 30% (B). Affording **ERNB** 22.6 mg. (Yield 44%). ^{1}H NMR (400 MHz, DMSO-d_6) δ 8.54 (t, J = 7.6 Hz, 2H), 8.41 (d, J = 8.4 Hz, 1H), 8.31 (d, J = 7.8 Hz, 2H), 7.88 (dt, J = 15.8, 7.7 Hz, 3H), 7.77 (t, J = 6.2 Hz, 1H), 7.70 (t, J = 7.5 Hz, 2H), 7.59 (d, J = 7.6 Hz, 2H), 7.24 (d, J = 7.8 Hz, 2H), 4.14 (t, J = 6.3 Hz, 2H), 3.12 (dd, J = 12.6, 6.3 Hz, 2H), 2.27 (s, 3H). ^{13}C NMR (100 MHz, DMSO-d_6) δ 164.73, 163.87, 163.36, 151.81, 142.95, 138.12, 135.14, 131.73, 131.68, 130.70, 129.95, 129.70, 129.18, 128.58, 128.41, 128.28, 126.82, 125.37, 123.09, 120.83, 120.70. 40.44, 39.84, 21.34. HRMS (ESI positive) calcd for $[M+H]^+$ 515.1271, found 515.1276. All the data were displayed in **Figure S6**-**S9**.

The fluorescence response of ERNB toward CES2. The fluorescence characteritics of **ERNB** toward CES2 were evaluated using our stander incubation system. Briefly, the *in vitro* assay system was performed in 100 mM potassium phosphate buffer (pH 7.4), with a final incubation volume of 0.2 mL. Firstly, potassium phosphate buffer, CES2 (the final concentration was 0.1 mg/mL) and 2 μL of the probe **ERNB** (the final concentration was 20 μM) was mixed, in order to avoid interference with the enzymes' catalytic activity the final concentration of DMSO did not exceed 1 % (*v/v*). Next, the sample was incubated at. 37 °C for 1 h, then, the reaction was terminated by the addition of 100 μL of acetonitrile and centrifged for 10 min at 4 °C with a centrifugal force of 20,000 × *g*. Then, the supernatant was used for fluorescence and HPLC analysis, respectively. Notably, control incubations without enzyme were performed in order to ensure that reaction was enzyme-dependent. For HPLC analysis we used the following method: the mobile phase consisted of methanol (A) and 0.03% trifluoroacetic acid water (B) at a flow rate of 0.8 mL/min. The following gradient conditions were used: 0 – 5 min 40% B; 5 – 15 min 40% – 15% B; 15 – 20 min 15% – 10% B; 20 – 25 min 10% – 40% B.

Selectivity of ERNB toward CES2. In order to confirm the selectity and stability of **ERNB**, **ERNB** was incubated with different hydrolases including: Ls, Cas, CES1, CES2, *β*-GLa, *β*-Glc, *β*-Glu and HSA in our standard incubation system, respectively. The final concentrations of all hydrolases were 8 μg/mL. Additionally, the fluorescence stability of **ERNB** with various exogenous substrates (Myristic acid, Serine, Tyrosine, Tryptophan, Glutamic acid, L-Arginine, Glycine, Glutamine, L(+)-Cysteine, Lysine, Glucose and Glutathione) as well as some common ions (Ni^{2+}, Mn^{2+}, Mg^{2+}, Ca^{2+}, Zn^{2+}, K^+, Sn^{4+}, Cu^{2+}, Na^+ , Fe^{3+}, SO_4^{2-}, CO_3^{2-}, Ba^{2+} and NO_3^-) were also evaluated, the final concentration of **ERNB** was 20 μM, all assays were conducted at 37 °C for 1 h. Then the data was analyzed using the Prism software package (GraphPad Software 7.0, LaJolla, CA).

Chemical inhibition and kinetic study. The Chemical inhibition was also performed in order to confirm the selectivity of **ERNB** for CES2, briefly, diffiient inhibitors Bis-p-nitrophenyl phosphate (BNPP, general inhibitor for CESs), Loperamide (LPA, CES2 selective inhibitor), Phenylbutazone (UGTs inhibitors), *α*-galactose (general inhibitor for glycosidases) were added in our incubation system with **ERNB**, respectively. Then, the residual activity was caculated by comparing with the control grop added DMSO. Furthermore, the kinetic of **ERNB** for CES2 over a concentration range from 0 – 180 μM was performed and the kinetic parameters were obtained.

The fluorescence imaging of CES2 in living cells. After the *in vitro* assay, the application of **ERNB** for fluorescence imaging was also evaluated. HepG2 cells were cultured in a DME/F-12 medium with 10% (*v/v*) fetal bovine serum (FBS) and 1% (*v/v*) antibiotics (penicillin/streptomycin) at 37 °C with 5% CO_2. At first, the cytotoxicity of **ERNB** was evaluated by the CCK-8 assay (Roche Diag-nosis, Indianapolis, IN). Briefly, HepG2 cells were seeded in a 96-well plate at a concentration of 8×10^3 /mL in culture medium and incubated overnight for attachment. Then different concentrations of **ERNB** (0, 1, 2, 5, 10, 20, 50, 100 μM) which was dissolved in FBS free culture medium was added to the 96-well plate, respectively. After 24 hours incubation, the culture medium was discarded and FBS free culture medium with 10% (*v/v*) CCK-8 was added for another one hour incubation in an incubator, and then detected at 450 nm using the Synergy H1 Reader (Bio-Tek). Then the cell viability was calculated and the group in the absence of **ERNB** was considered as 100%.

For the fluorescence imaging, briefly, HepG2 cells were seeded on 20-mm glass polylysine-coated confocal cell culture dishes and attached overnight. Next day, after discarding the culture medium, a medium containing 80 μM of **ERNB** was added to the cluture cells and incubated at 37 °C for 1 h. In addition a control group with the same volume of blank solvent. After the incubation, the cells were washed with 37 °C PBS (pH 7.4) three times. Then cells were imaged using a confocal microscope (Leica TCS SP8) with an excitation wavelength at 405 nm and the fluorescence signal in the blue channel (425 – 475 nm) and green channel (535 – 585 nm) were recorded, respectively. Then, the imaging ratio was calculated from green/blue. Simultaneously, the CES2 selective inhibitor LPA (50 μM) was pre-treated for 30 min and then **ERNB** was added for chemical inhibition in living cells. The purpose was to confirm that the fluorescence signal was generated by CES2 in HepG2 cells.

The fluorescence imaging in tissues by ERNB. In view of the good imaging characteritics of **ERNB**, we applyed **ERNB** for tissue fluorescence imaging. In detail, 10 μm frozen tissue slices were prepared from the cancer tissues of HepG2 bearing nude mice. All protocols for this animal study conformed to the Guide for the Care and Use of Laboratory Animals. All animal experiments were performed in accordance with guidelines approved by the ethics committee of Dalian Medical University (the protocol registry number: AEE17030). The slices were incubated with **ERNB** (50 μM) at 37 °C for 1 h followed by washing the slices three times with PBS. Subsequently, the stained samples with **ERNB** were examined with a Leica TCS SP8 confocal microscope the conditions were the same as those used cell imaging.

Co-localization Imaging in Living Cells. The co-localization imaging in HepG2 cells was performed to explore whether **ERNB** could target the endoplasmic reticulum, due to the probe **ERNB** generating a significant increase in the green channel, we stained the ER using a commicial tracker Red (BODIPY® TR Glibenclamide). The staining procedures were performed following the instructions of the tracker and the **ERNB** was just added as above. Additionally, mitochondrial and lysosome tracker were also added, respectively. Then, the cells were imaged by the laser confocal microscope.

The CES2 changes under ER Stress. At first, after the attachment of HepG2 cells overnight the classic ER stress inducer DTT (5 mM) and tunicamycin (20 μg/mL) was added into the cells and incubated for 60 min and 5 h, respectively. Then, **ERNB** was added into the cells and incubated for another 1 hour. Then, the cells were imaged using a confocal microscope (Leica TCS SP8) with an excitation wavelength of 405 nm and different fluorescence channel signals were collected as previously described. Using the above experiments, our aim is to illustrate the change of CES2 activity at the ER under ER stress and give some useful guidance for the diagnosis and therapy of diseases involved in ER stress.

The CES2 regulation in a drug-induced acute liver injury model. We estabilished a drug-induced acute liver injury model using APAP (acetaminophen) at a dose of 400 mg/kg; briefly, male C57BL/6J mice were randomly separated into the following two groups: control (saline, ip); APAP only (400 mg/kg, ip); they were executed after being treated with APAP (400 mg/kg) for 12 h, the serum and liver tissues were obtained for the biochemical analysis Alanine aminotransferase (ALT) and Aspartate aminotransferase (AST) and pathological examination (H & E staining). All protocols for this animal study conformed to the Guide for the Care and Use of Laboratory Animals. All animal experiments were performed in accordance with guidelines approved by the ethics committee of Dalian Medical University (the protocol registry number: AEE17030). Additionally, the frozen liver slices were prepared and imaged using **ERNB** to observe the activity change of CES2 in ER stress animal model, the procedures were as described above for tissue imaging. Furthermore, the change of the CES2 expression was also assayed using western blot.

RESULTS AND DISCUSSIONS

Spectroscopic change of ERNB toward CES2. Firstly, the absorption and fluorescence properties of **ERNB** toward CES2 were investigated. As shown in **Figure 1 A-B**, **ERNB** displayed a maximum absorption at 350 nm, and a new absorption peak at 450 nm was observed after incubation with CES2, the same results were also observed for the substrate **ERNB** and metabolite **ERNH** (**Figure S10**). In addition the fluorescence intensity at 560 nm increased along with a decrease in fluorescence intensity at 414 nm, HPLC analysis indicated that CES2 catalyzed the hydrolysis of **ERNB** to **ERNH** (**Figure S11**). We then observed the fluorescence changes of **ERNB** toward CES2 at different protein concentration, as shown in **Figure 1 C-D**, the fluorescence intensity ratio I_{560}/I_{414} exhibited good linearity over a range of CES2 concentrations (0 – 8 μg/mL). These results indicate that **ERNB** can be used to monitor CES2 activity in complex bio-samples.

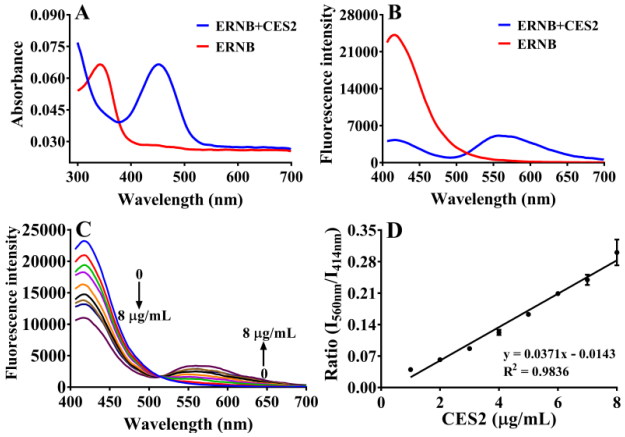

Figure 1 The absorption (A) and emission (B) spectral response of **ERNB** (20 μM) toward CES2; (C, D) linear response of **ERNB** toward different concentration of CES2 over a range from 0 – 8 μg/mL. λ_{ex} = 380 nm.

Selectivity of ERNB. The selectivity of **ERNB** toward CES2 was evaluated, as shown in **Figure 2 A**, after incubation with different hydrolases including Ls, *β*-Glc, Cas, CES1, CES2, HSA, *β*-Gla, *β*-Glu, only CES2 could trigger the hydrolysis reaction, and the catalytic activity was much higher than CES1. Furthermore, **ERNB** showed good stability toward common endogenous substrates and metal ions including Ser, Glu, Trp, Cys, Arg, Cys, Lys, Gly, Gln, myristic acid, GSH, Glucose, Ca^{2+}, Mg^{2+}, Mn^{2+}, Ni^{2+}, Sn^{4+}, K^{+}, Cu^{2+}, Zn^{2+}, Na^{+}, Fe^{3+}, CO_3^{2-}, NO^{3-} and Ba^{2+}, facilitating the use of **ERNB** in living systems (**Figure 2 B**). Additionally, during the chemical assay only CES general inhibitor bis-*p*-nitrophenyl phosphate (BNPP) and CES2 selective inhibitor loperamide (LPA) could significantly inhibit the reaction in HLM, which further suggested that **ERNB** hydrolysis was selectively catalyzed by CES2, (**Figure 2 C**). The result was consistent with the substrate preferences of CES2 that it mainly recognizes substrates with large alcohol and small acyl group, such as irinotecan. Good kinetic behavior with enzymes is vital for activity-based fluorescent probes. **Figure 2D** indicates that **ERNB** follows a classic Michaelis-Menton kinetic model with CES2, the kinetic parameters K_m and V_{max} are 3.48 ± 0.61 μM and 0.027 ± 0.001 nmol/min/μg, respectively. K_m is equal to the substrate concentration at which the reaction rate is half its maximal value, thus, our results indicate that **ERNB** has high selectivity and affinity toward CES2, excellent kinetic performance, making **ERNB** a suitable tool for quantifying CES2 activity in complex biological samples.

Fluorescence imaging of CES2 in living cells and tissues. We then explored the use of **ERNB** for imaging endogenous CES2 in living cells and tissues. Firstly, the CCK8 assay indicated that **ERNB** was not cytotoxic up to 100 μM (**Figure S12**). Secondly, in **Figure 3**, after incubation with **ERNB** for 1 h, a fluorescence signal at 425 – 475 nm was observed clearly indicating that **ERNB** could cross the cell membrane smoothly; a new fluorescence signal at 535 – 585 nm was detected, and the ratio (green/blue) was calculated to be 2.4 which indicated that CES2 expressed in HepG2 cells and mediated the generation of a fluorescence signal in the green

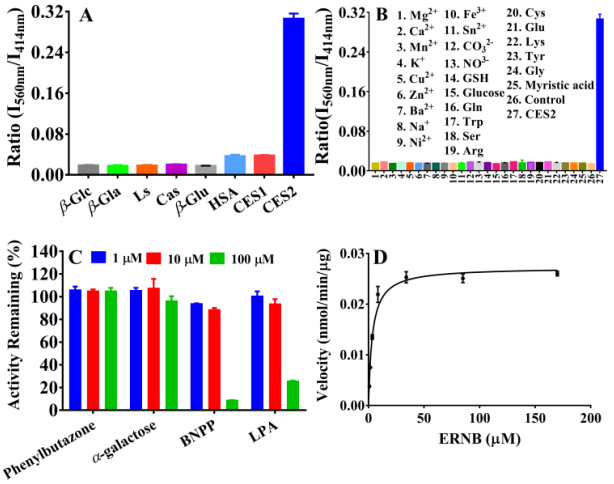

Figure 2. (A) The selectivity of **ERNB** amongst various hydrolases; (B) the stability of **ERNB** towards diffident amino acids and metal ions; (C) the chemical inhibition of different selective inhibitors towards **ERNB** reaction in HLM (Human liver microsome) system; (D) kinetic model of **ERNB** with CES2.

channel, while control HepG2 cells produced no fluorescence signal under the same conditions (**Figure S13**). Additionally, HepG2 cells pre-incubated with the CES2 inhibitor LPA (50 μM) displayed reduced fluorescence intensity in the green channel and the fluorescence intensity ratio decreased to 0.88, these results indicated that the fluorescence signal was dependent on intracellular CES2 expression. Additionally, the expression of CES2 in tumor tissues prepared from the cancer tissues of HepG2 bearing nude mice was also investigated. As shown in **Figure S14**, significant fluorescence in the blue and green channels was detected in HepG2 tissues, and high ratio values indicating an abundant expression of CES2 in HepG2 cells.

Co-localization imaging of CES2 by ERNB. After the systematic assay of **ERNB** including response, selectivity, linear range, stability and imaging in living cells, we further explored the subcellular localization of CES2 in living cells. As shown in **Figure 4**, HepG2 cells were co-incubated with

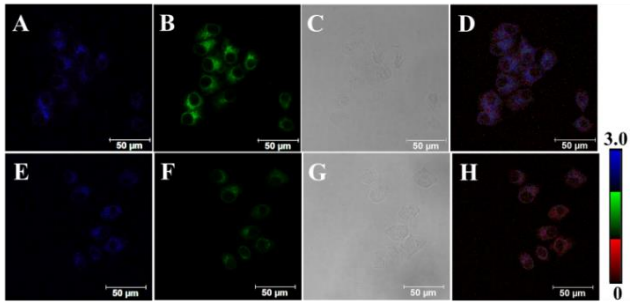

Figure 3. (A，B) The fluorescence imaging of CES2 in HepG2 cells at different channel (Blue: 425 – 475 nm; Green: 535 – 585 nm) after incubation with **ERNB** (100 μM); (E, F) the HepG2 cell preincubated with CES2 selective inhibitor LPA (50 μM); (C, G) the bright field images of HepG2 cells; (D, H) F_{green}/F_{blue} intensity ratios. Scale bars 50 μm.

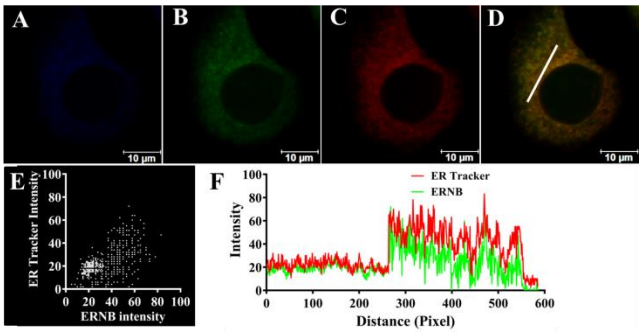

Figure 4. (A) Fluorescence images of of **ERNB** in HepG2 at the blue channel (425 – 475 nm); (B) fluorescence images of of **ERNB** in HepG2 at the green channel (535 – 585 nm); (C) ER-Tracker (red); (D) merged fluorescence image of the green channel and ER-Tracker channel (red); (E) intensity scatter plot; (F) fluorescence intensity for region of interest (white line in panel D). Scale bars 10 μm.

ERNB and commercial ER-Tracker (Red) then imaged using a confocal fluorescence microscope. As expected, the fluorescence overlapped (**Figure 4D**) and the green fluorescence signal produced by **ERNB** correlated well with the commercial ER-Tracker red signal and the Pearson's correlation was calculated to be 0.96. Additionally, **ERNB** displayed almost no fluorescence inside the mitochondria (**Figure S15**) and lysosome (**Figure S16**), respectively. All these results indicated that **ERNB** could image endogenous CES2 in living systems and exclusively target the ER which is useful for the evaluation of CES2 changes and regulation under ER stress and some ER-related diseases.

CES2 regulation under ER Stress. ER stress is a common condition for diseases such as diabetes, neurodegenerative disease, ischemia/reperfusion injury, hypoxia, and drug-induced toxicology which can result in cell death. CES2 is a major phase I metabolic enzyme which is mainly expressed at the ER. Importantly, in our work, the activity changes of CES2 under ER stress could be evaluated using **ERNB**. As shown in **Figure 5**, after treatment with DTT (DL-dithiothreitol, an acknowledged ER stress inducer),[37,38] the CES2 activity exhibited a sharp decrease which was reflected by a reduced fluorescence intensity ratio compared to the control group (0.79 *vs* 2.34). The same effect was observed in the tunicamycin-induced ER stress system (**Figure S17**).[39,40] All these results indicated that the activity of CES2 was reduced under ER stress.

Detection of CES2 in APAP-induced acute liver injury model

In order to further confirm the variation of CES2 activity under ER stress, an acetaminophen (APAP)-induced acute liver injury model was established which was accompanied by ER stress.[41-44] As shown in **Figure 6 A-D**, after treatment with APAP 400 mg/kg for 12 h, the liver surface was rough with many hepatic parenchymal injury areas, and the index of liver function enzyme ALT displayed a 23-fold increase, as well as 3-fold increase of AST, all these results indicate that an acute liver injury model has been established, additionally, the large area tissue necrosis in the H & E staining confirmed liver injury (**Figure S18**). Subsequently, frozen tissue slices of the

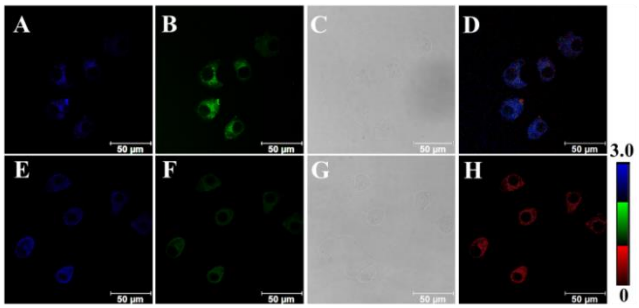

Figure 5. (A, B) The fluorescence imaging of HepG2 cells after incubation with **ERNB**; (E, F) the imaging of CES2 after treatment with DTT (5 mM) for 1 h; (C, G) the bright field of HepG2 cells; (D, H) F_{green}/F_{blue} intensity ratios. Scale bar is 50 μm.

liver were prepared from the APAP treated and control groups respectively, and then incubated with **ERNB** (50 μM) for 1 h. As shown in **Figure 6 E – J**, the APAP treated group gave a very weak fluorescence signal in the green channel and lower ratio values compared with the control. These results further confirmed the decrease of CES2 activity in drug-induced acute liver injury. Additionally, a western blot assay indicated a down-regulation of CES2 activity under ER stress which was consistent with the imaging results using **ERNB** (**Figure 6 K**).

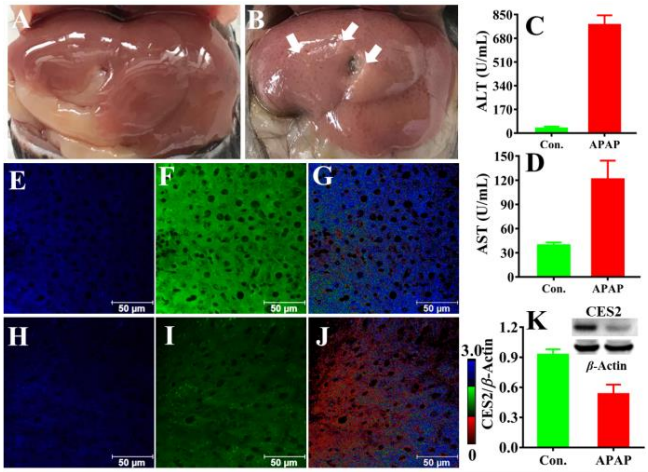

Figure 6. The bright field of liver of normal (A) and APAP-induced group (B); (C) the serum ALT assay for normal and APAP-treatment group; (D) the serum AST assay for normal and APAP treatment group; (E, F) fluorescence imaging of CES2 in normal liver tissue; (H, I) CES2 imaging in APAP-induced acute liver injury tissue; (G, J) F_{green}/F_{blue} intensity ratios; (K) Western blot assay of CES2 in normal and APAP-induced liver.

CONCLUSIONS

In summary, in order to monitor CES2 activity under ER stress, we developed a novel stable ER-targeting ratiometric fluorescent probe named **ERNB** with high selectivity and sensitivity for application *in vitro* and in living systems. The fluorescence intensity ratio (I_{560}/I_{414}) displayed excellent dependence on CES2 activity. In addition, **ERNB** was used for real-time evaluation of endogenous CES2 changes under ER stress in living HepG2 cells and drug-induced acute liver injury

models. Our results indicate a significant decrease in CES2 activity and expression under ER stress. Therefore, **ERNB** can serve as a useful tool for elucidating the role of CES2 in the ER and can be used to follow the bio-functions of ER stress associated diseases.

ASSOCIATED CONTENT

Supporting Information

Synthetic procedures, NMR, HRMS-characterization, and Supplementary Figures for the experiments. The Supporting Information is available free of charge on the ACS Publications website.

AUTHOR INFORMATION

*Corresponding Author

E-mail addresses: maxc1978@163.com (X. Ma), leifeng@mail.dlut.edu.cn (L. Feng), and t.d.james@bath.ac.uk (T. D. James)

Author Contributions

[#] These authors contributed equally.

Notes

The authors declare no competing financial interests.

ACKNOWLEDGMENTS

The authors thank the National Natural Science Foundation of China (81930112, 81622047 and 81503201), National Key R&D Program of China (2018YFC1705900), State Key Laboratory of Fine Chemicals (KF1803), Distinguished Professor of Liaoning Province program and Liaoning Revitalization Talents Program for financial support. TDJ wishes to thank the Royal Society for a Wolfson Research Merit Award.

REFERENCES

(1) Satoh, T.; Taylor, P.; Bosron, W. F.; Sanghani, S. P.; Hosokawa, M.; La Du, B. N. Current progress on esterases: from molecular structure to function. *Drug Metab. Dispos.* **2002**, *30*, 488-493.

(2) Imai, T. Human carboxylesterase isozymes: catalytic properties and rational drug design. *Drug Metab. Pharmacokinet.* **2006**, *21*, 173-185.

(3) Li, Y.; Zalzala, M.; Jadhav, K.; Xu, Y.; Kasumov, T.; Yin, L.; Zhang, Y. Carboxylesterase 2 prevents liver steatosis by modulating lipolysis, endoplasmic reticulum stress, and lipogenesis and is regulated by hepatocyte nuclear factor 4 alpha in mice. *Hepatology* **2016**, *63*, 1860-1874.

(4) Ruby, M. A.; Massart, J.; Hunerdosse, D. M.; Schonke, M.; Correia, J. C.; Louie, S. M.; Ruas, J. L.; Naslund, E.; Nomura, D. K.; Zierath, J. R. Human carboxylesterase 2 reverses obesity-induced diacylglycerol accumulation and glucose intolerance. *Cell Rep.* **2017**, *18*, 636-646.

(5) Imai, T.; Ohura, K. The role of intestinal carboxylesterase in the oral absorption of prodrugs. *Curr. Drug Metab.* **2010**, *11*, 793-805.

(6) Shimizu, M.; Fukami, T.; Nakajima, M.; Yokoi, T. Screening of specific inhibitors for human carboxylesterases or arylacetamide deacetylase. *Drug Metab. Dispos.* **2014**, *42*, 1103-1109.

(7) Cui, Y.; Tian, X.; Ning, J.; Wang, C.; Yu, Z.; Wang, Y.; Huo, X.; Jin, L.; Deng, S.; Zhang, B.; Ma, X. Metabolic profile of 3-acetyl-11-keto-beta-boswellic acid and 11-keto-beta-boswellic acid in human preparations in vitro, species differences, and bioactivity variation. *AAPS J.* **2016**, *18*, 1273-1288.

(8) Ashraf, N. U.; Sheikh, T. A. Endoplasmic reticulum stress and oxidative stress in the pathogenesis of non-alcoholic fatty liver disease. *Free Radic. Res.* **2015**, *49*, 1405-1418.

(9) Foufelle, F.; Fromenty, B. Role of endoplasmic reticulum stress in drug-induced toxicity. *Pharmacol. Res. Perspect.* **2016**, *4*, e00211.

(10) Michalak, M. Quality control in the endoplasmic reticulum. *Semin. Cell Dev. Biol.* **2010**, *21*, 471.

(11) Cybulsky, A. V. Endoplasmic reticulum stress, the unfolded protein response and autophagy in kidney diseases. *Nat. Rev. Nephrol.* **2017**, *13*, 681-696.

(12) Liao, Y.; Hussain, T.; Liu, C.; Cui, Y.; Wang, J.; Yao, J.; Chen, H.; Song, Y.; Sabir, N.; Hussain, M.; Zhao, D.; Zhou, X. Endoplasmic reticulum stress induces macrophages to produce IL-1beta during mycobacterium bovis infection via a positive feedback loop between mitochondrial damage and inflammasome activation. *Front Immunol.* **2019**, *10*, 268.

(13) Yilmaz, E. Endoplasmic reticulum stress and obesity. *Adv. Exp. Med. Biol.* **2017**, *960*, 261-276.

(14) Thornton, C.; Baburamani, A. A.; Kichev, A.; Hagberg, H. Oxidative stress and endoplasmic reticulum (ER) stress in the development of neonatal hypoxic-ischaemic brain injury. *Biochem. Soc. Trans.* **2017**, *45*, 1067-1076.

(15) Hotamisligil, G. S. Endoplasmic reticulum stress and the inflammatory basis of metabolic disease. *Cell* **2010**, *140*, 900-917.

(16) Xu, C.; Bailly-Maitre, B.; Reed, J. C. Endoplasmic reticulum stress: cell life and death decisions. *J. Clin. Invest.* **2005**, *115*, 2656-2664.

(17) Rao, R. V.; Bredesen, D. E. Misfolded proteins, endoplasmic reticulum stress and neurodegeneration. *Curr. Opin. Cell Biol.* **2004**, *16*, 653-662.

(18) Zeng, L.; Zeng, H.; Jiang, L.; Wang, S.; Hou, J.-T.; Yoon, J. A Single Fluorescent Chemosensor for Simultaneous Discriminative Detection of Gaseous Phosgene and a Nerve Agent Mimic. *Anal. Chem.* **2019**, 91, 12070-12076.

(19) Ning, J.; Wang, W.; Ge, G.; Chu, P.; Long, F.; Yang, Y.; Peng, Y.; Feng, L.; Ma, X.; James, T. D. Target Enzyme-Activated Two-Photon Fluorescent Probes: A Case Study of CYP3A4 Using a Two-Dimensional Design Strategy. *Angew. Chem. Int. Ed.* **2019**, *58*, 9959-9963.

(20) Jin, Y.; Tian, X.; Jin, L.; Cui, Y.; Liu, T.; Yu, Z.; Huo, X.; Cui, J.; Sun, C.; Wang, C.; Ning, J.; Zhang, B.; Feng, L.; Ma, X. Highly specific near-infrared fluorescent probe for the real-time detection of beta-glucuronidase in various living cells and animals. *Anal. Chem.* **2018**, *90*, 3276-3283.

(21) Dou, K.; Chen, G.; Yu, F.; Liu, Y.; Chen, L.; Cao, Z.; Chen, T.; Li, Y.; You, J. Bright and sensitive ratiometric fluorescent probe enabling endogenous FA imaging and mechanistic exploration of indirect oxidative damage due to FA in various living systems. *Chem. Sci.* **2017**, *8*, 7851-7861.

(22) Ning, J.; Liu, T.; Dong, P.; Wang, W.; Ge, G.; Wang, B.; Yu, Z.; Shi, L.; Tian, X.; Huo, X.; Feng, L.; Wang, C.; Sun, C.; Cui, J.; James, T. D.; Ma, X. Molecular design strategy to construct the near-infrared fluorescent probe for selectively sensing human cytochrome P450 2J2. *J. Am. Chem. Soc.* **2019**, *141*, 1126-1134.

(23) Duan, C.; Won, M.; Verwilst, P.; Xu, J.; Kim, H. S.; Zeng, L.; Kim, J. S. In Vivo Imaging of Endogenously Produced HClO in Zebrafish and Mice Using a Bright, Photostable Ratiometric Fluorescent Probe. *Anal. Chem.* **2019**, 91, 4172-4178.

(24) Liu, H. W.; Chen, L.; Xu, C.; Li, Z.; Zhang, H.; Zhang, X. B.; Tan, W. Recent progresses in small-molecule enzymatic fluorescent probes for cancer imaging. *Chem. Soc. Rev.* **2018**, *47*, 7140-7180.

(25) Zhang, J.; Chai, X.; He, X. P.; Kim, H. J.; Yoon, J.; Tian, H. Fluorogenic probes for disease-relevant enzymes. *Chem. Soc. Rev.* **2019**, *48*, 683-722.

(26) Feng L.; Ning J.; Tian X.; Wang C.; Zhang L.; Ma X.; James T.; Fluorescent probes for bioactive detection and imaging of phase II metabolic enzymes. *Coord. Chem. Rev*. **2019**, DOI: doi.org/10.1016/j.ccr.2019.213026.

(27) Jiang, A.; Chen, G.; Xu, J.; Liu, Y.; Zhao, G.; Liu, Z.; Chen, T.; Li, Y.; James, T. D. Ratiometric two-photon fluorescent probe for in situ imaging of carboxylesterase (CE)-mediated mitochondrial acidification during medication. *Chem. Commun.* **2019**, doi: 10.1039/C9CC05759E.

(28) Yan, Z.; Wang, J.; Zhang, Y.; Zhang, S.; Qiao, J.; Zhang, X. An iridium complex-based probe for photoluminescence lifetime imaging of human carboxylesterase 2 in living cells. *Chem. Commun.* **2018**, *54*, 9027-9030.

(29) Feng, L.; Liu, Z. M.; Hou, J.; Lv, X.; Ning, J.; Ge, G. B.; Cui, J. N.; Yang, L. A highly selective fluorescent ESIPT probe for the detection of human carboxylesterase 2 and its biological applications. *Biosens. Bioelectron.* **2015**, *65*, 9-15.

(30) Liu, Z. M.; Feng, L.; Hou, J.; Lv, X.; Ning, J.; Ge, G.-B.; Wang, K.-W.; Cui, J. N.; Yang, L. A ratiometric fluorescent sensor for highly selective detection of human carboxylesterase 2 and its application in living cells. *Sens. Actuators, B.* **2014**, *205*, 151-157.

(31) Feng, L.; Liu, Z. M.; Xu, L.; Lv, X.; Ning, J.; Hou, J.; Ge, G. B.; Cui, J. N.; Yang, L. A highly selective long-wavelength fluorescent probe for

the detection of human carboxylesterase 2 and its biomedical applications. *Chem. Commun.* **2014**, *50*, 14519-14522.
(32) Wang, J.; Williams, E. T.; Bourgea, J.; Wong, Y. N.; Patten, C. J. Characterization of recombinant human carboxylesterases: fluorescein diacetate as a probe substrate for human carboxylesterase 2. *Drug Metab. Dispos.* **2011**, *39*, 1329-1333.
(33) Hou, J. T.; Kim, H. S.; Duan, C.; Ji, M. S.; Wang, S.; Zeng, L.; Ren, W. X.; Kim, J. S. A ratiometric fluorescent probe for detecting hypochlorite in the endoplasmic reticulum. *Chem. Commun.* **2019**, *55*, 2533-2536.
(34) Xu, S.; Liu, H. W.; Hu, X. X.; Huan, S. Y.; Zhang, J.; Liu, Y. C.; Yuan, L.; Qu, F. L.; Zhang, X. B.; Tan, W. Visualization of endoplasmic reticulum aminopeptidase 1 under different redox conditions with a two-photon fluorescent probe. *Anal. Chem.* **2017**, *89*, 7641-7648.
(35) Xiao, H.; Wu, C.; Li, P.; Gao, W.; Zhang, W.; Zhang, W.; Tong, L.; Tang, B. Ratiometric photoacoustic imaging of endoplasmic reticulum polarity in injured liver tissues of diabetic mice. *Chem. Sci.* **2017**, *8*, 7025-7030.
(36) Xiao, H.; Liu, X.; Wu, C.; Wu, Y.; Li, P.; Guo, X.; Tang, B. A new endoplasmic reticulum-targeted two-photon fluorescent probe for imaging of superoxide anion in diabetic mice. *Biosens. Bioelectron.* **2017**, *91*, 449-455.
(37) Cheng, Z.; Rendleman, J.; Vogel, C. Time-course proteomics dataset monitoring HeLa cells subjected to DTT induced endoplasmic reticulum stress. *Data Brief* **2016**, *8*, 1168-1172.
(38) Oslowski, C. M.; Urano, F. Measuring ER stress and the unfolded protein response using mammalian tissue culture system. *Methods Enzymol.* **2011**, *490*, 71-92.
(39) Li, S. J.; Zhou, D. Y.; Li, Y.; Liu, H. W.; Wu, P.; Ou-Yang, J.; Jiang, W. L.; Li, C. Y. Efficient two-photon fluorescent probe for imaging of nitric oxide during endoplasmic reticulum stress. *ACS Sens.* **2018**, *3*, 2311-2319.
(40) Xiao, H. B.; Zhang, R. L.; Wu, C. C.; Li, P.; Zhang, W.; Tang, B. A new pH-sensitive fluorescent probe for visualization of endoplasmic reticulum acidification during stress. *Sens. Actuators, B.* **2018**, *273*, 1754-1761.
(41) Kusama, H.; Kon, K.; Ikejima, K.; Arai, K.; Aoyama, T.; Uchiyama, A.; Yamashina, S.; Watanabe, S. Sodium 4-phenylbutyric acid prevents murine acetaminophen hepatotoxicity by minimizing endoplasmic reticulum stress. *J. Gastroenterol.* **2017**, *52*, 611-622.
(42) Kalinec, G. M.; Thein, P.; Parsa, A.; Yorgason, J.; Luxford, W.; Urrutia, R.; Kalinec, F. Acetaminophen and NAPQI are toxic to auditory cells via oxidative and endoplasmic reticulum stress-dependent pathways. *Hear. Res.* **2014**, *313*, 26-37.
(43) Lee, D. H.; Lee, B.; Park, J. S.; Lee, Y. S.; Kim, J. H.; Cho, Y.; Jo, Y.; Kim, H. S.; Lee, Y. H.; Nam, K. T.; Bae, S. H. Inactivation of sirtuin2 protects mice from acetaminophen-induced liver injury: possible involvement of ER stress and S6K1 activation. *BMB Rep.* **2019,** 52: 190-195.
(44) Nagy, G.; Kardon, T.; Wunderlich, L.; Szarka, A.; Kiss, A.; Schaff, Z.; Banhegyi, G.; Mandl, J. Acetaminophen induces ER dependent signaling in mouse liver. *Arch. Biochem. Biophys.* **2007**, *459*, 273-279.

Table of Contents (TOC):